

## Original Research Article

# Proteomics analysis of differentially-expressed proteins in uterus of primary dysmenorrhea mice following administration of nuangong zhitong

Yazhen Xie<sup>1,2</sup>, Jianqiang Qian<sup>2</sup>, Qibin Lu<sup>3\*</sup>

<sup>1</sup>Nanjing University of Chinese Medicine, Nanjing, <sup>2</sup>Taicang Traditional Chinese Medicine Hospital Affiliated to Nanjing University of Chinese Medicine, Taicang, <sup>3</sup>Department of Gynaecology, The Affiliated Hospital of Nanjing University of Chinese Medicine, Nanjing, Jiangsu, PR China

\*For correspondence: **Email:** xyz8102@sina.com; **Tel:** +86 25 8661 7141

Sent for review: 23 July 2019

Revised accepted: 27 January 2020

### Abstract

**Purpose:** To use label-free proteomic method to investigate the mechanism of action of nuangong zhitong decoction (NZD) on primary dysmenorrhea (PD).

**Methods:** A mouse model of PD was established through oxytocin administration. The mice were divided into control group (normal mice), model group (PD mice administered normal saline), and treatment group (mice given NZD). The serum levels of PGE<sub>2</sub> and PGF<sub>2</sub> $\alpha$  in the mice were measured by ELISA. The differentially expressed proteins (DEPs) among the three groups were revealed by identifying the proteins that were up-regulated (or down-regulated) in model group and down-regulated (or up-regulated) in the treatment group. The DEPs in the three groups were identified using Nano-HPLC-MS/MS, and their functions were investigated using bioinformatics analyses. The accuracy of proteomics was verified with western blot analysis.

**Results:** Thirty-eight up-regulated and 66 down-regulated DEPs were identified. Bioinformatics analysis revealed that the DEPs were related to immune response, signal conduction, protein binding, and metabolism. STRING analysis indicated a total of 53 DEPs have direct or indirect functional links. Western blot results revealed that levels of Stat1, Rock1, vinculin and caveolin-1 were consistent with the results of proteomic analysis.

**Conclusion:** These findings provide further insights into the mechanism underlying the protective effects of NZD.

**Keywords:** Primary dysmenorrhea, Uterus, Nuangong zhitong decoction, Vinculin, Caveolin, Differentially expressed proteins (DEPs), Bioinformatics

This is an Open Access article that uses a fund-ing model which does not charge readers or their institutions for access and distributed under the terms of the Creative Commons Attribution License (<http://creativecommons.org/licenses/by/4.0>) and the Budapest Open Access Initiative (<http://www.budapestopenaccessinitiative.org/read>), which permit unrestricted use, distribution, and reproduction in any medium, provided the original work is properly credited.

Tropical Journal of Pharmaceutical Research is indexed by Science Citation Index (SciSearch), Scopus, International Pharmaceutical Abstract, Chemical Abstracts, Embase, Index Copernicus, EBSCO, African Index Medicus, JournalSeek, Journal Citation Reports/Science Edition, Directory of Open Access Journals (DOAJ), African Journal Online, Bioline International, Open-J-Gate and Pharmacy Abstracts

## INTRODUCTION

Primary dysmenorrhea (PD) refers to recurrent menstrual cramps that are not due to other diseases. It occurs in approximately 50% of

menstruating females. The pain associated with PD is extremely severe in 15% of patients, and results in psychological distress such as anxiety and depression [1]. Moreover, PD pain may be accompanied with nausea-and-vomiting, fatigue, and diarrhea [3]. Currently, the principal

pharmacological therapies for PD include oral contraceptives and non-steroidal anti-inflammatory drugs (NSAIDs). [4]. However, these drugs are associated with adverse side effects [5]. Thus, in their place, Chinese herbal medicine is used for treating PD due to its fewer adverse effects and lower degree of PD recurrence [6,7].

*Nuangong zhitong* decoction (NZD) has been used for clinical treatment of PD for many years in China. It was developed from the traditional Chinese prescription of *Wen jing* decoction which has been used clinically treating dysmenorrhea for decades. [8]. *Nuangong zhitong* decoction (NZD) is composed of *Cinnamomi ramulus*, *evodiamine*, *asarum*, *Radix linderae* and *rhizoma corydalis* at the ratio of 1:2:1:2:2. Cinnamaldehyde and cinnamic acid are the two main constituents of *Cinnamomi ramulus*. They have been reported to suppress oxytocin-induced uterine contractions [9,10]. Evodiamine, *asarum*, *Radix linderae* and *rhizoma corydalis* warm the meridians so as to dissipate cold and relieve pain. However, the molecular mechanisms that underlie the analgesic effect of NZD are poorly understood. Therefore, there is need for more studies in this area.

Label-free quantitative proteomics has been employed to explore the mechanisms of medicine, including traditional Chinese Medicine (TCM) [11-14]. It emerged as a powerful approach for large-scale protein analysis with quantifying peptides and proteins with the use of a peptide's response as a quantitative measure [15,16]. In this study, proteomic alterations in PD mice in response to NZD treatment were investigated using Nano-HPLC-MS/MS technology.

## EXPERIMENTAL

### Animal model of PD

Animal experiments in this study were approved by Ethics Committee of Taicang TCM Hospital Affiliated to Nanjing University of Traditional Chinese Medicine. Female KM mice (mean weight = 25 ± 5 g, 6 – 8 weeks of age) were purchased from Cavens Laboratory Animal Co. Ltd (Changzhou, China). The mice were intragastrically administered a decoction made from gypsum, gentiana, *Phellodendron chinense* and *Rhizoma anemarrhena*, mixed in a ratio 2:1.2:1:1.5, at a dose of 4 g/mL for 14 days to establish a mouse model of cold-type asthenia. The mice were then subcutaneously injected with estradiol benzoate injection (2 mg/kg) daily for 12 days to improve the sensitivity of the mice uterine

tissues to oxytocin. On the 12<sup>th</sup> day, oxytocin (20 U/kg) was injected intraperitoneally to the mice to induce severe uterine contraction.

Seven days after establishment of ACT-PD model, the mice were randomly divided into 2 groups (10 mice/group) administered normal saline (model group) or NZD at a dose of 30.00 g/kg body weight (bwt, treatment group) for another 7 days. Ten (10) healthy Balb/c mice which were intragastrically administered normal saline for 13 days (10 mL/kg bwt) served as control group. On the 13<sup>th</sup> day, writhing reaction was induced through intraperitoneal injection of oxytocin (33 U/kg).

### Writhing test

The mice were placed in a box and intraperitoneally injected with oxytocin. The number of writhes in 30 min was counted. Analgesia (A) was calculated according to Eq 1.

$$A (\%) = \{(WPD - Wt)/WPD\} \dots\dots\dots (1)$$

where  $W_{PD}$  and  $W_t$  are the no. of writhes in PD and treatment groups, respectively

### Enzyme-linked immunosorbent assay (ELISA)

Blood was collected from the retroorbital plexus of mice after administration of NZD or its bioactive components for 40 min. The serum levels of PGE2 and PGF2 $\alpha$  were measured with ELISA kits according to the kit protocol.

### Sample preparation and protein digestion

There were three samples of mouse uterus tissue in each group. After cutting them into smaller pieces, RIPA lysis buffer was added, and the tissues were mechanically homogenized using a tissue homogenizer thrice, each for 3 sec. After an incubation of 15 min on ice, the samples were centrifuged at 12,000 g for 15 min at 4°C, and the supernatants were separately transferred into new Eppendorf tubes. BCA assay was used for the detection of the protein concentration of the supernatant. Proteins were diluted with 8 M urea solution followed by a further incubation of 1 h at 37°C. Thereafter, the mixture was transferred into 10 K Microcon centrifugal filter unit (Millipore, Billerica, MA). The samples were centrifuged to remove urea. The proteins were then alkylated by iodoacetamide at room temperature for 20 min (in the dark) and digested with sequence-grade modified trypsin (Promega) and lyophilized.

## LCMS/MS analysis

Solvent A (0.1% formic acid, 30  $\mu$ L) was used for resuspending peptides. Separations were performed with an EASY-nano-LC 1200 system (Thermo Fisher Scientific). Peptide sample (6  $\mu$ L) was loaded into a trap column (C18, 75  $\mu$ m x 2 cm, flow rate: 300 nL/min), and subsequently separated and loaded onto an analytical column (C18, 75  $\mu$ m x 50 cm) using a linear gradient of 5–38% B (0.1% formic acid in ACN) for 120 min. A 2 kV electrospray voltage between the sprayer and ion inlet of the mass spectrometer was utilized in the study.

## Identification of DEPs

PEAKS Studio (version 8.5, Bioinformatics Solutions Inc., Waterloo, Canada) was used to analyze tandem mass spectra. PEAKS DB was used to search the UniProt-mouse database (ver.201711, 52194 entries). The search parameters were 0.05 and 7 ppm for the fragment and parent ions mass tolerances, respectively. The fixed modification was carbamidomethylation (C), while the variable modifications were deamidation (NQ), oxidation (M), and acetylation (Protein N-term). Peptides were filtered with 1% FDR and 1 unique. The abundance of peptide and protein was calculated using ANOVA. The averaging the abundance of all peptides was normalization using medians. Protein with fold-changes over 1.5 and at least 2 unique peptides with significance over 13 ( $p < 0.05$ ) was considered to be a Differently-expressed protein (DEP).

## Bioinformatics analysis

The obtained DEPs were analyzed using three databases: Kyoto Encyclopedia of Genes and Genomes (KEGG), Gene Ontology (GO), and the Clusters of Orthologous Groups (KOGs) databases. The interaction network of DEPs was built with the STRING.

## Western blot analysis

Uterus tissue from each mouse was used to

extract protein using RIPA lysis buffer containing 1% PMSF and cocktail (Beyotime, Haimen, China). BCA assay was employed to estimate the protein concentration. The protein was separated by 8–10% SDS-PAGE and transferred to polyvinylidene difluoride (PVDF) membranes. After blocking with non-fat milk (5%), the membranes were then incubated overnight with anti-vinculin, anti-caveolin, anti-stat1, anti-rock1 and anti-GAPDH at 4 °C. The membranes were washed thrice with TBST buffer and then incubated with secondary antibodies at room temperature for 1 h. Enhanced chemiluminescence (ECL) reagent (Thermo Fisher Scientific, Inc.) was used for the detection of interest protein bands. Image J v1.48u software (National Institutes of Health, Bethesda, MD, USA) was employed to analyze the relative optical densities of interest bands.

## Statistical analysis

Statistical analysis was performed with SPSS 19.0 software (IBM Corp., NY). All data are expressed as mean  $\pm$  standard deviation (SD). The differences between two groups were analyzed by Student's *t*-test. One-way ANOVA was used for multiple-group comparisons. Statistical significance was assumed at  $p < 0.05$ .

## RESULTS

### Effect of NZD on writhing in primary dysmenorrhea

As shown in Table 1, compared with the control mice, a remarkable increased number of writhes was observed in model mice, indicating the successful establishment of PD model. Treatment with NZD significantly reduced the number of writhes ( $p < 0.01$ ), and the percentage analgesia was 61.82. Model mice showed significant increases in the levels of serum PGE2 and PGF2 $\alpha$ . However, administration of NZD induced a remarkable decrease in the levels of PGE2 and PGF2 $\alpha$  ( $p < 0.01$ ). These findings suggest that NZD can significantly relieve PD.

**Table 1:** Effect of NZD on writhing reaction, analgesia and serum PGE2 and PGF2 $\alpha$  levels of PD model mice

Group	Number of writhes in 30 min	Analgesia (%)	PGE2 (pg/mL)	PGF2 $\alpha$ (pg/mL)
Control	0.00 $\pm$ 0.00	100.00	70.60 $\pm$ 19.31	239.46 $\pm$ 27.41
Model	61.30 $\pm$ 9.56**	0.00	142.80 $\pm$ 12.79**	718.27 $\pm$ 35.07**
Treatment	23.40 $\pm$ 13.60##	61.82	35.40 $\pm$ 15.01###	317.87 $\pm$ 72.28##

\*\* $p < 0.01$ , compared to control group; ## $p < 0.01$ , compared to model group (n=10).

### Identification of DEPs in uterus of PD mice administered NZD

Nano-HPLC-MS/MS was applied to identify DEPs in uterine tissues in the three groups. As shown in Table 2, a total of 556 DEPs were identified between control group and model group, out of which 245 were up-regulated, while 311 were down-regulated. Four hundred and four (404) DEPs were identified between the model group and treatment group, 238 of which were up-regulated, while 166 were down-regulated. There were 471 DEPs between the control group and the treatment group, with 267 up-regulated and 204 down-regulated. The DEPs among the three groups were then further analyzed via identification of the up-regulated or down-regulated proteins in model and treatment groups. Sixty-six proteins were up-regulated in model group and down-regulated in treatment group, while 38 proteins which were down-regulated in model group were up-regulated in treatment group. These results are displayed in Table 3.

### GO analysis

To extract information relevant to involved pathways of DEPs, the protein data obtained were analyzed using DAVID network analysis tool. Moreover, GO analysis was carried out on cellular components (CC), molecular functions (MF), and biological processes (BPs) associated with the DEPs. In the BP analysis, majority of DEPs were associated with immune response, immune system process, regulation of localization and single-organism transport (Figure 1). The CC analysis showed that most of DEPs were present in the cytoplasm (Figure 1). Molecular functional classification of DEPs showed that DEPs were mainly involved in protein binding, catalytic activity and hydrolase activity (Figure 1).

### KEGG pathway analysis

The results of KEGG analysis revealed that the DEPs were significantly associated with

tuberculosis, *Staphylococcus aureus* infection, leukocyte transendothelial migration and phagosome. The results also indicated that the DEPs were associated with Parkinson's disease, Fc gamma R-mediated phagocytosis and chemokine signaling pathway (Figure 2).

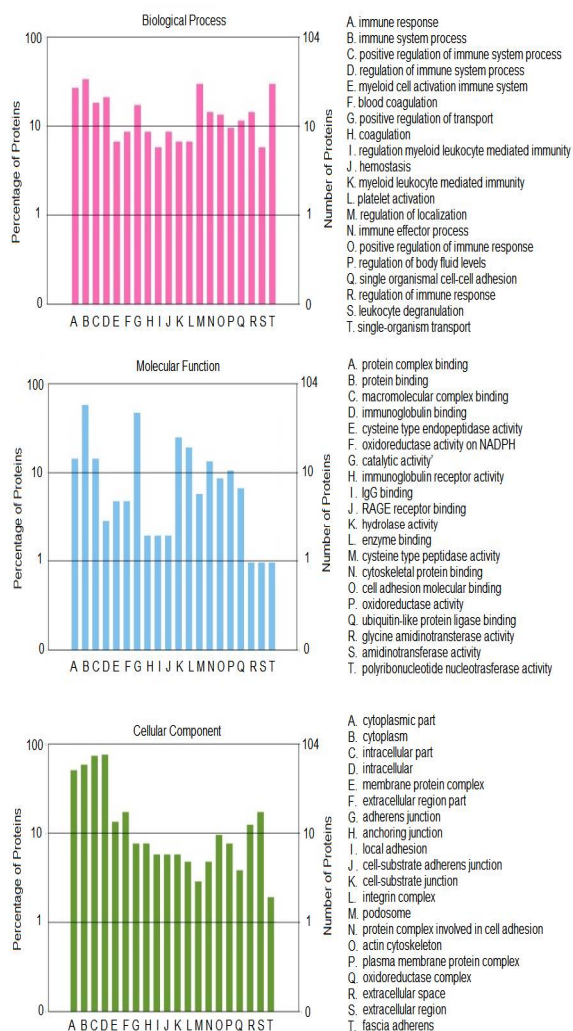


**Figure 1:** GO annotation of DEPs in biological process (BP), cellular component (CC) and molecular function (MF)

**Table 2:** Number of DEP in uteruses of control, model and treatment groups

Group	Number of DEPs	Number of up-regulated proteins	Number of down-regulated proteins
Control group vs model group	556	245	311
Model group vs treatment group	404	238	166
Control group vs treatment group	471	267	204

**Table 3:** Comparison of differentially-expressed proteins (DEPs) in uterus among control, model and treatment groups

Uniprot accession no.	Protein description	Gene symbol	Fold change ratio		P		Tendency	
			A	B	A	B	A	B
E9QPE7	Myosin-11	Myh11	0.437	1.563	0.038	0.048	Do	Up
P31001	Desmin	Des	0.488	1.845	0.011	0.008	Do	Up
E9PZ16	Basement membrane-specific heparan sulfate proteoglycan core protein	Hspg2	0.397	1.652	0.029	0.037	Do	Up
Q80X90	Filamin-B	Flnb	1.813	0.633	0.009	0.008	Up	Do
Q9JJZ2	Tubulin alpha-8 chain	Tuba8	1.614	0.382	0.031	0.048	Up	Do
Q64727	Vinculin	Vcl	0.663	1.755	0.037	0.042	Do	Up
E9PV24	Fibrinogen alpha chain	Fga	1.912	0.483	0.011	0.019	Up	Do
Q61233	Plastin-2	Lcp1	2.013	0.423	0.006	0.008	Up	Do
P00920	Carbonic anhydrase 2	Ca2	1.914	0.659	0.033	0.045	Up	Do
P51661	Corticosteroid 11-beta-dehydrogenase isozyme 2	Hsd11b2	0.421	1.606	0.036	0.048	Do	Up
P97449	Aminopeptidase N	Anpep	0.388	1.563	0.015	0.018	Do	Up
P01029	Complement C4-B	C4b	1.214	0.437	0.031	0.040	Up	Do
A0A0R4J1B4	Integrin alpha-M	Itgam	2.131	0.590	0.001	0.004	Up	Do
Q9D379	Epoxide hydrolase 1	Ephx1	0.294	1.970	0.006	0.018	Do	Up
P25688	Uricase	Uox	2.114	0.576	0.032	0.041	Up	Do
Q8C3V4	Signal transducer and activator of transcription	Stat1	1.985	0.438	0.003	0.002	Up	Do
P16125	L-lactate dehydrogenase B chain	Ldhb	0.214	1.597	0.002	0.003	Do	Up
P14873	Microtubule-associated protein 1B	Map1b	0.564	1.811	0.041	0.048	Do	Up
P01865	Ig gamma-2A chain C region	Igh-1a	1.354	0.623	0.039	0.045	Up	Do
P30681	High mobility group protein B2	Hmgb2	1.974	0.647	0.019	0.026	Up	Do
Q61599	Rho GDP-dissociation inhibitor 2	Arhgdib	2.231	0.459	0.015	0.010	Up	Do
Q54218	Integrin beta	Itgb2	2.223	0.545	0.009	0.010	Up	Do
P68037	Ubiquitin-conjugating enzyme E2 L3	Ube2l3	1.991	0.623	0.025	0.038	Up	Do
Q05144	Ras-related C3 botulinum toxin substrate 2	Rac2	2.412	0.447	0.001	0.004	Up	Do
Q9CZS1	Aldehyde dehydrogenase X mitochondrial	Aldh1b1	0.477	4.196	0.026	0.010	Do	Up
Q8K1B8	Fermitin family homolog 3	Fermt3	1.876	0.484	0.031	0.021	Up	Do

**Table 3:** Comparison of differentially-expressed proteins (DEPs) in uterus among control, model and treatment groups

Uniprot accession no.	Protein description	Gene symbol	Fold change ratio		P		Tendency	
			A	B	A	B	A	B
Q9ESB3	Histidine-rich glycoprotein	Hrg	2.223	0.549	0.008	0.011	Up	Do
A0A171EBL2	E3 ubiquitin-protein ligase RNF213	Rnf213	1.968	0.362	0.012	0.014	Up	Do
P25911	Tyrosine-protein kinase Lyn	Lyn	1.963	0.597	0.015	0.017	Up	Do
P43275	Histone H1.1	Hist1h1a	2.218	0.576	0.007	0.010	Up	Do
P49817	Caveolin-1	Cav1	0.254	2.009	0.008	0.006	Do	Up
P35385	Heat shock protein beta-7	Hspb7	0.873	2.011	0.038	0.045	Do	Up
S4R1M0	Receptor-type tyrosine-protein phosphatase C	Ptpcr	1.752	0.414	0.024	0.030	Up	Do
Q61093	Cytochrome b-245 heavy chain 1	Cybb	2.014	0.536	0.001	0.002	Up	Do
e	Basic leucine zipper and W2 domain-containing protein 2	Bzw2	0.374	1.598	0.001	0.002	Do	Up
P97821	Dipeptidyl peptidase 1	Ctsc	1.797	0.495	0.012	0.016	Up	Do
e	Long-chain-fatty-acid--CoA ligase 3	Acs13	1.895	0.585	0.011	0.010	Up	Do
e	NADH dehydrogenase [ubiquinone] 1 alpha subcomplex subunit 10 mitochondrial	Ndufa10	0.373	1.623	0.003	0.005	Do	Up
Q9Z0P5	Twinfilin-2	Twf2	1.987	0.639	0.019	0.024	Up	Do
Q8K1J6	CCA tRNA nucleotidyltransferase 1 mitochondrial	Trnt1	2.013	0.487	0.017	0.022	Up	Do
Q60770	Syntaxin-binding protein 3	Stxbp3	0.434	1.601	0.029	0.034	Do	Up
Q7TMF3	NADH dehydrogenase [ubiquinone] 1 alpha subcomplex subunit 12	Ndufa12	0.383	1.552	0.025	0.038	Do	Up
G3UW94	MCG14259 isoform CRA_b	U2af1	1.646	0.473	0.034	0.045	Up	Do
P56695	Wolframin	Wfs1	0.593	1.668	0.019	0.035	Do	Up
Q8K124	Pleckstrin homology domain-containing family O member 2	Plekho2	2.015	0.475	0.002	0.004	Up	Do
O35744	Chitinase-like protein 3	Chil3	1.030	0.199	0.041	0.047	Up	Do
P49710	Hematopoietic lineage cell-specific protein	Hcls1	1.717	0.428	0.009	0.011	Up	Do
Q80WQ2	Protein VAC14 homolog	Vac14	0.252	1.644	0.011	0.024	Do	Up
Q9D964	Glycine amidinotransferase mitochondrial	Gatm	2.556	0.494	0.001	0.000	Up	Do
O09117	Synaptophysin-like protein 1	Sypl1	0.686	2.134	0.024	0.039	Do	Up
O89017	Legumain	Lgmn	1.881	0.5900	0.018	0.010	Up	Do
P97426	Eosinophil cationic protein 1	Ear1	1.667	0.598	0.027	0.038	Up	Do
A0A0B4J1G1	Fc receptor IgG low affinity IIb	Fcgr2b	1.737	0.286	0.008	0.006	Up	Do
e	Large proline-rich protein BAG6	Bag6	1.223	0.619	0.041	0.037	Up	Do
Q8BLY1	SPARC-related modular calcium-binding protein 1	Smoc1	0.667	2.390	0.039	0.049	Do	Up

**Table 3:** Comparison of differentially-expressed proteins (DEPs) in uterus among control, model and treatment groups

Uniprot accession no.	Protein description	Gene symbol	Fold change ratio		P		Tendency	
			A	B	A	B	A	B
P70335	Rho-associated protein kinase 1	Rock1	1.414	0.377	0.018	0.027	Up	Do
Q9D1J3	SAP domain-containing ribonucleoprotein	Sarnp	1.919	0.654	0.018	0.022	Up	Do
Q8BYA0	Tubulin-specific chaperone D	Tbcd	0.626	2.160	0.028	0.005	Do	Up
Q07456	Protein AMBP	Ambp	1.558	0.534	0.029	0.033	Up	Do
G5E814	MCG5603	Ndufa11	1.663	0.578	0.021	0.018	Up	Do
O35601	FYN-binding protein 1	Fyb1	1.364	0.580	0.037	0.049	Up	Do
O70370	Cathepsin S	Ctss	1.414	0.428	0.031	0.029	Up	Do
Q3UIR3	E3 ubiquitin-protein ligase DTX3L	Dtx3l	1.818	0.643	0.022	0.036	Up	Do
Q60648	Ganglioside GM2 activator	Gm2a	0.418	2.159	0.026	0.043	Do	Up
Q6P9Q6	FK506-binding protein 15	Fkbp15	2.073	0.617	0.011	0.019	Up	Do
Q8BWZ3	N-alpha-acetyltransferase 25 NatB auxiliary subunit	Naa25	0.593	1.827	0.007	0.011	Do	Up
O89110	Caspase-8	Casp8	2.141	0.559	0.002	0.005	Up	Do
Q78J03	Methionine-R-sulfoxide reductase B2	Msrb2	0.492	1.972	0.023	0.037	Do	Up
P31725	Protein S100-A9	S100a9	2.015	0.378	0.009	0.014	Up	Do
A2APF7	Z-DNA-binding protein 1	Zbp1	2.221	0.306	0.001	0.007	Up	Do
Q91Z40	Gbp6 protein	Gbp7	1.823	0.324	0.021	0.018	Up	Do
Q9JHK5	Pleckstrin	Plek	1.973	0.552	0.010	0.017	Up	Do
Q9R0P9	Ubiquitin carboxyl-terminal hydrolase isozyme L1	Uchl1	0.545	2.039	0.013	0.027	Do	Up
Q8BPU7	Engulfment and cell motility protein 1	Elmo1	1.662	0.357	0.022	0.043	Up	Do
A2AP32	NADH dehydrogenase [ubiquinone] 1 beta subcomplex subunit 6	Ndufb6	0.587	4.531	0.035	0.008	Do	Up
Q3ULD5	Methylcrotonoyl-CoA carboxylase beta chain	Mccc2	0.212	1.703	0.003	0.006	Do	Up
O70200	Allograft inflammatory factor 1	Aif1	2.313	0.509	0.002	0.010	Up	Do
Q9QXD8	LIM domain-containing protein 1	Limd1	2.432	0.657	0.000	0.004	Up	Do
Q8C3J5	Dedicator of cytokinesis protein 2	Dock2	1.373	0.149	0.011	0.040	Up	Do
Q99LI7	Cleavage stimulation factor subunit 3	Cstf3	0.245	1.940	0.032	0.028	Do	Up
Q3UVK0	Endoplasmic reticulum metalloproteinase 1	Ermp1	1.562	0.665	0.014	0.017	Up	Do
Q02105	Complement C1q subcomponent subunit C	C1qc	1.636	0.485	0.019	0.028	Up	Do
P57787	Monocarboxylate transporter 4	Slc16a3	1.921	0.511	0.021	0.013	Up	Do
Q9R1J0	Sterol-4-alpha-carboxylate 3-dehydrogenase decarboxylating	Nsdhl	2.015	0.636	0.014	0.026	Up	Do
Q64282	Interferon-induced protein with tetratricopeptide repeats 1	Ifit1	1.999	0.262	0.004	0.008	Up	Do
P56376	Acylphosphatase-1	Acyp1	0.565	1.708	0.009	0.011	Do	Up
e	Nuclear autoantigen Sp-100	Sp100	1.838	0.568	0.004	0.007	Up	Do

**Table 3:** Comparison of differentially-expressed proteins (DEPs) in uterus among control, model and treatment groups

Uniprot accession no.	Protein description	Gene symbol	Fold change ratio		P		Tendency	
			A	B	A	B	A	B
Q9DB73	NADH-cytochrome b5 reductase 1	Cyb5r1	0.445	2.416	0.010	0.025	Do	Up
Q03963	Interferon-induced double-stranded RNA-activated protein kinase	Eif2ak2	1.844	0.546	0.027	0.039	Up	Do
Q91VN4	MICOS complex subunit Mic25	Chchd6	0.461	1.724	0.013	0.025	Do	Up
P20491	High affinity immunoglobulin epsilon receptor subunit gamma	Fcer1g	1.525	0.484	0.023	0.015	Up	Do
Q8BUK6	Protein Hook homolog 3	Hook3	0.915	2.178	0.038	0.046	Do	Up
Q62084	Protein phosphatase 1 regulatory subunit 14B	Ppp1r14b	0.321	1.717	0.034	0.029	Do	Up
Q9EQ32	Phosphoinositide 3-kinase adapter protein 1	Pik3ap1	2.156	0.243	0.000	0.002	Up	Do
Q8K1R3	Polyribonucleotide nucleotidyltransferase 1	Pnpt1	0.858	7.289	0.001	0.004	Do	Up
Q91Z50	Flap endonuclease 1	Fen1	1.752	0.411	0.016	0.026	Up	Do
e	FYVE and coiled-coil domain-containing protein 1	Fyco1	1.842	0.354	0.037	0.024	Up	Do
Q9Z1Q2	Protein ABHD16A	Abhd16a	0.553	1.541	0.021	0.012	Do	Up
Q5SWD9	Pre-rRNA-processing protein TSR1 homolog	Tsr1	0.663	1.917	0.041	0.040	Do	Up
Q8C0Z1	Protein FAM234A	Fam234	0.515	2.496	0.009	0.002	Do	Up
P13597	Intercellular adhesion molecule 1	Icam1	1.641	0.218	0.031	0.029	Up	Do
e	Protein THEMIS2	Themis2	1.717	0.431	0.019	0.025	Up	Do
Q9R099	Transducin beta-like protein 2	Tbl2	0.373	2.090	0.011	0.019	Do	Up
P26151	High affinity immunoglobulin gamma Fc receptor I	Fcgr1	1.565	0.290	0.018	0.029	Up	Do

A: comparison of control group and model group; B: comparison of model group and treatment group. Up = up-regulation; Do = down-regulation.

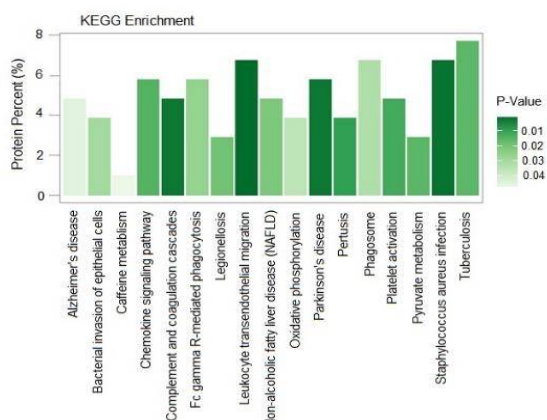


**Figure 2:** Distribution of enriched KEGG pathway. Columns represents related pathways. Midnight green represents smaller *p* values) and lighter green represents bigger *p* values

**KOGs analysis**

The results of KOGs analysis showed that the functions of the DEPs were mostly in information storage and processing, cellular processes and signaling, and metabolism (Figure 3). The results indicated that these processes may be involved in the therapeutic effect of NZD.

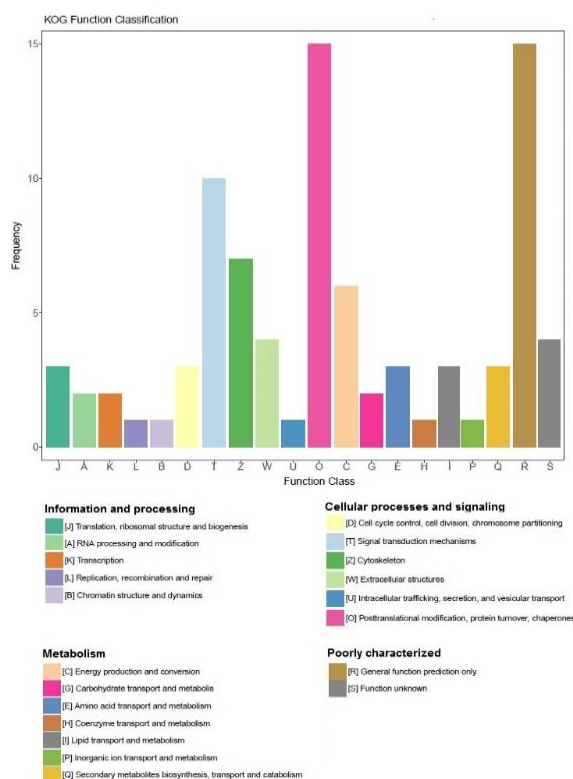


**Figure 3:** KOGs analysis of DEPs. The different colored columns refer to different functions. The frequency of proteins enriched in the function refer to the value of the ordinate.

**PPI analysis**

For further exploring the mechanisms involved in the protective effect of NZD, STRING database was used to construct the PPI network of the DEPs. As shown in Figures 4, a total of 53 DEPs in the map have direct or indirect links.

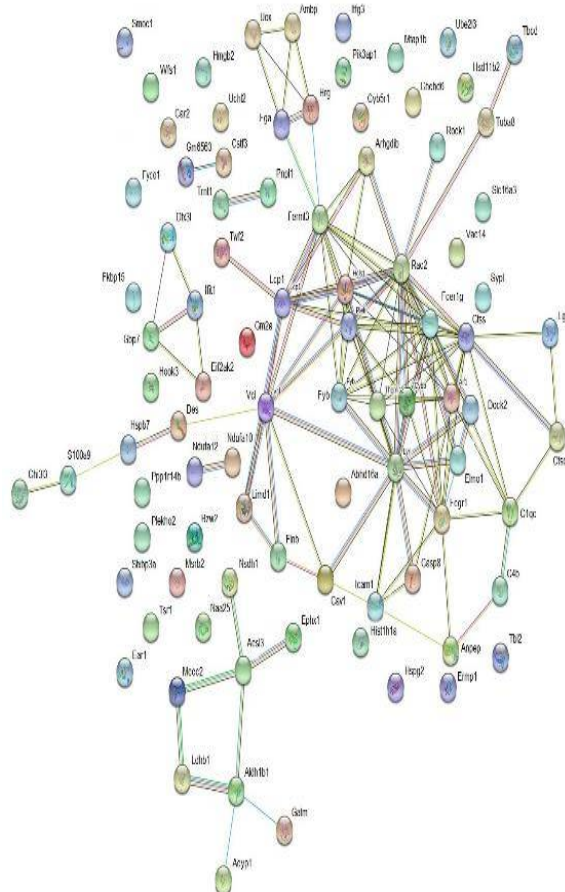


**Figure 4:** Interaction networks of DEPs. Protein association network of the DEPs were constructed after searching STRING database with a confidence cutoff of 0.6. Proteins are indicated by nodes. Thickness of lines represents the confidence level (0.6 – 0.9).

**Validation by western blot on DEPs**

As shown in Fig.5, the expression levels of Stat1 and Rock1 were significantly elevated in model group and down-regulated in treatment group, while vinculin and caveolin-1 showed significant decreases in model group and increases in treatment group. These results were consistent with the observations in proteomics analysis.

**DISCUSSION**

Although NZD has been used in China to treat PD in clinics for many years, the underlying

mechanism remains largely unknown. To the best of the authors' knowledge, the present study is the first to use label-free proteomic based method to investigate the mechanism of NZD on a PD model. The results showed that NZD reduced oxytocin-induced writhing response after oxytocin injection in PD mice. The serum levels of PGE2 and PGF2 $\alpha$ , which are regarded as the most critical pain factors in PD [17], were significantly decreased after NZD administration. These findings suggest that NZD exerts a significant analgesic effect in PD mice.

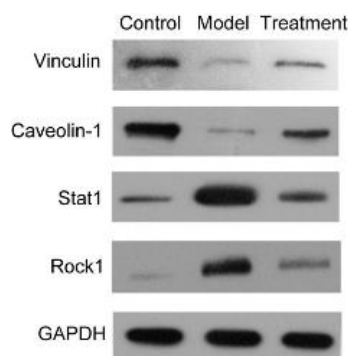


**Figure 5:** Western blot analysis confirmed DEPs initially identified using quantitative proteomics method. The expressions of vinculin, caveolin-1, Stat1 and Rock1 in uteruses of mice in the three groups were analyzed using western blot, with GAPDH as the loading control

Label-free quantitative proteomics is useful in searching for disease-associated factors and has been used to investigate the mechanism of TCM in recent years [11-14]. The present study identified 38 up-regulated DEPs and 66 down-regulated DEPs after NZD treatment. The GO and KEGG analyses revealed significant alteration of functions and signaling pathways in PD mice after NZD administration. These changes affected protein binding, immune response, catalytic activity and chemokine signaling pathway. These GOs and pathways may play important roles in the analgesic action of NZD. The results of KOGs analysis revealed that the functions of the DEPs mainly involved in metabolism, cellular processes and signaling, information storage and processing.

The accuracy of proteomics was verified using western blotting with respect to the expressions of vinculin, caveolin-1, Stat1 and Rock1 in the three groups. The levels of Stat1 and Rock1 in uteruses were elevated in model group and down-regulated in treatment group. Vinculin and caveolin-1 showed decreases in model group and increases in treatment group. These results confirmed the credibility of proteomic analysis.

## CONCLUSION

The proteomic studies in the present investigation have revealed a number of DEPs involved in the response to NZD administration in PD mice. It is hoped that these findings will provide a database resource for further investigations on the mechanisms involved in the protective effect of NZD against PD.

## DECLARATIONS

### Acknowledgement

This work was supported by the Project of Taicang Science and Technology (no. TC2017YYJC03).

### Conflict of interest

No conflict of interest is associated with this work

### Contribution of authors

We declare that this work was done by the authors named in this article, and all liabilities pertaining to claims relating to the content of this article will be borne by the authors. Qi-Bin Lu designed all the experiments and revised the manuscript. Ya-Zhen Xie and Jian-Qiang Qian performed the experiments, while Ya-Zhen Xie wrote the manuscript.

### Open Access

This is an Open Access article that uses a funding model which does not charge readers or their institutions for access and distributed under the terms of the Creative Commons Attribution License (<http://creativecommons.org/licenses/by/4.0>) and the Budapest Open Access Initiative (<http://www.budapestopenaccessinitiative.org/read>), which permit unrestricted use, distribution, and reproduction in any medium, provided the original work is properly credited.

## REFERENCES

1. Rencz F, Pentek M, Stalmeier PFM, Brodszky V, Ruzsa G, Gradwohl E, Baji P, Gulacsi L. Bleeding out the quality-adjusted life years: evaluating the burden of primary dysmenorrhea using time trade-off and willingness-to-pay methods. *Pain* 2017; 158(11): 2259-2267.
2. Suvitie P. Dysmenorrhea in teenagers. *Duodecim* 2017; 133(3): 285-291.
3. Payne LA, Rapkin AJ, Seidman LC, Zeltzer LK, Tsao JC. Experimental and procedural pain responses in primary  
*Trop J Pharm Res, February 2020; 19(2): 274*

- dysmenorrhea: a systematic review. *J Pain Res* 2017; 10: 2233-2246.
4. Bernardi M, Lazzeri L, Perelli F, Reis FM, Petraglia F. Dysmenorrhea and related disorders. *F1000Res* 2017; 6: 1645.
  5. Davis AR, Westhoff C, O'Connell K, Gallagher N. Oral contraceptives for dysmenorrhea in adolescent girls: a randomized trial. *Obstet Gynecol* 2005; 106(1): 97-104.
  6. Nazar H, Usmanghani K. Clinical evaluation to assess the safety and efficacy of coded herbal medicine "Dysmo-off" versus allopathic medicine "Diclofenac sodium" for the treatment of primary dysmenorrhea. *J Herb Pharmacother* 2006; 6(1): 21-39.
  7. Oya A, Oikawa T, Nakai A, Takeshita T, Hanawa T. Clinical efficacy of Kampo medicine (Japanese traditional herbal medicine) in the treatment of primary dysmenorrhea. *J Obstet Gynaecol Res* 2008; 34(5): 898-908.
  8. Gao L, Jia C, Zhang H, Ma C. Wenjing decoction (herbal medicine) for the treatment of primary dysmenorrhea: a systematic review and meta-analysis. *Arch Gynecol Obstet* 2017; 296(4): 679-689.
  9. He DY, Dai SM. Anti-inflammatory and immunomodulatory effects of paeonia lactiflora pall. a traditional chinese herbal medicine. *Front Pharmacol* 2011; 2: 10.
  10. Sun L, Liu L, Zong S, Wang Z, Zhou J, Xu Z, Ding G, Xiao W, Kou J. Traditional Chinese medicine Guizhi Fuling capsule used for therapy of dysmenorrhea via attenuating uterus contraction. *J Ethnopharmacol* 2016; 191: 273-279.
  11. Lee JH, Kim DH, Song WK, Oh MK, Ko DK. Label-free imaging and quantitative chemical analysis of Alzheimer's disease brain samples with multimodal multiphoton nonlinear optical microspectroscopy. *J Biomed Opt* 2015; 20(5): 56013.
  12. Luczak M, Suszynska-Zajczyk J, Marczak L, Formanowicz D, Pawliczak E, Wanic-Kossowska M, Stobiecki M. Label-Free Quantitative Proteomics Reveals Differences in Molecular Mechanism of Atherosclerosis Related and Non-Related to Chronic Kidney Disease. *Int J Mol Sci* 2016; 17(5).
  13. Bostanci N, Selevsek N, Wolski W, Grossmann J, Bao K, Wahlander A, Trachsel C, Schlapbach R, Öztürk VÖ, Afacan B et al. Targeted Proteomics Guided by Label-free Quantitative Proteome Analysis in Saliva Reveal Transition Signatures from Health to Periodontal Disease. *Mol Cell Proteomics* 2018; 17(7): 1392-1409.
  14. Zhang Y, Zhan C, Chen G, Sun J. Label-free quantitative proteomics and bioinformatics analyses of alcoholic liver disease in a chronic and binge mouse model. *Mol Med Rep* 2018; 18(2): 2079-2087.
  15. Patel VJ, Thalassinou K, Slade SE, Connolly JB, Crombie A, Murrell JC, Scrivens JH. A comparison of labeling and label-free mass spectrometry-based proteomics approaches. *J Proteome Res* 2009; 8(7): 3752-3759.
  16. Bantscheff M, Lemeer S, Savitski MM, Kuster B. Quantitative mass spectrometry in proteomics: critical review update from 2007 to the present. *Anal Bioanal Chem* 2012; 404(4): 939-965.
  17. Powell AM, Chan WY, Alvin P, Litt IF. Menstrual-PGF2 alpha, PGE2 and TXA2 in normal and dysmenorrheic women and their temporal relationship to dysmenorrhea. *Prostaglandins* 1985; 29(2): 273-290.